# Solution of the inverse scattering problem in specular reflection

R. Lipperheide and G. Reiss
*Hahn-Meitner-Institut Berlin and Freie Universität Berlin, Postfach 390128, D-14091 Berlin, Germany*

H. Leeb
*Institut für Kernphysik, Technische Universität Wien, A-1040 Vienna, Austria*

H. Fiedeldey* and S. A. Sofianos
*Department of Physics, University of South Africa, P.O. Box 392, Pretoria 0001, South Africa*
(Received 8 August 1994)

One-dimensional inversion is applied to neutron specular reflection for a model-independent determination of the scattering-length density profile. The Marchenko equation for complex potentials is solved directly, as well as via the Neumann series and the Padé approximant. As part of the input information of the inverse problem for complex potentials, a formula is derived for the reflection coefficient at negative incident momenta.

## I. INTRODUCTION

Cold and ultracold neutrons behave like electromagnetic waves, and their scattering is described by neutron optics.[1] Such neutrons are used to investigate the structure of surfaces and interfaces of samples in the nanometer range.[2–5]

If the samples are planar we have to do with specular reflection and transmission. This is essentially quantal scattering by a one-dimensional potential barrier representing the scattering-length density profile of the sample. The determination of this potential from the scattering information then is the one-dimensional inverse scattering problem. Usually one has recourse to a simulation, i.e., one chooses a model for the potential whose parameters are adjusted via a fit to the data. However, for an unambiguous, model-independent answer one should solve the inverse scattering problem in its true mathematical sense. We mention in parentheses that in x-ray and electron scattering this is often called the direct method,[6] by which is meant that the solution of the inverse scattering problem is sought directly, not indirectly by simulation. As neutron (and x-ray) reflection becomes a more widely used technique to probe the profile of surfaces and thin films, the need for inverse scattering calculations will increase. This point has been made and developed in Refs. 4 and 7–14, where various types of inversion schemes have also been proposed.

The general mathematical formalism for solving the one-dimensional inverse scattering problem was developed long ago;[15–19] it is based on the Marchenko integral equation. However, practical applications have been made only recently. They have mostly been concerned with special classes of solvable potentials, which are associated with degenerate kernels of the Marchenko equation. Such potentials have been used, e.g., in the nuclear inverse scattering problem at fixed angular momentum,[20,21] or for optical wave guides[22] and ionospheric-structure investigations.[23] A particular version of the solvable-potentials method has been discussed in Refs. 24 and 25. The Marchenko equation with nondegenerate kernels has been solved for real potentials up to the first few terms in the Neumann series in an application to fluids,[26] and more recently in an essentially exact, modified form in Refs. 27 and 28.

The present paper is devoted to a general solution of the Marchenko equation for both real and complex potentials. We consider only potentials which support no bound states, as in the case in most applications. The Marchenko equation is solved directly, and also by the Neumann series and the Padé approximant. Schematic examples are given for steplike profiles, i.e., for samples mounted on an infinitely thick substrate, as well as for complex potentials (absorptive materials).

## II. THE MARCHENKO EQUATION AND ITS SOLUTION

Consider a potential $V(x)$ with $V(x)=0$ for $x<0$ and (in general) $V(x)\to V_s$ for $x\to\infty$, which yields a left reflection coefficient $R_-(q)$ as a solution of the direct scattering problem at incident momentum $q$. The potential can in turn be obtained from the reflection coefficient as the solution of the inverse scattering problem. This is done in the following manner:[15,17] First, one calculates the Fourier transform $B(x)$ of the reflection coefficient $R_-(q)$, $B(x)=0$ for $x<0$ and

$$B(x)=\frac{1}{2\pi}\int_{-\infty}^{\infty} dq\, e^{-iqx}R_-(q) \quad \text{for } x>0\ . \tag{1}$$

This quantity serves as input in the Marchenko integral equation

$$K(x,y)+B(x+y)+\lambda\int_{-x}^{x} dz\, B(z+y)K(x,z)=0 \quad \text{with } x>y\ . \tag{2}$$

The strength parameter $\lambda$ has been introduced here in order to facilitate the construction of the Neumann series;

 

one eventually sets $\lambda=1$. From the solutions of Eq. (2) one obtains the potential as $V(x)=0$ for $x<0$ and

$$V(x)=2\frac{dK(x,x-0)}{dx} \quad \text{for } x>0 \ . \tag{3}$$

The integral equation (2) is a Fredholm equation in the variables $y,z$ for fixed values of $x$. It can be solved (i) directly, or (ii) by making use of a finite Neumann series which is given by the first $M+1$ terms of the expansion of the solution $K(x,y)$ in the parameter $\lambda$:

$$\begin{aligned} K^{(\mathrm{Neu})}(x,y)&=\sum_{n=0}^{M}\lambda^n K_n(x,y) \ , \\ K_0(x,y)&=-B(x+y) \ , \\ K_n(x,y)&=-\int_{-x}^{x} dz\, K_{n-1}(x,z)B(z+y) \\ &\qquad \text{for } n=1,\ldots,M \ . \end{aligned} \tag{4}$$

The condition for the convergence of the Neumann series is

$$\|B\|_x^2\equiv\int_{-x}^{x}\int_{-x}^{x}|B(y+z)|^2 dy\, dz<1 \ . \tag{5}$$

If this condition is not satisfied, we may consider (iii) the $(N,N)$ Padé approximant,[29,30] which has the form

$$K^{(\mathrm{Pade})}(x,y)=\frac{\sum_{n=0}^{N}\lambda^n C_n(x,y)}{1+\sum_{n=1}^{N}\lambda^n D_n(x,y)} \ . \tag{6}$$

For any fixed pair of variables $(x,y)$ the coefficients $C_n$ and $D_n$ are determined from the terms $K_n=K_n(x,y)$ by the equations

$$\sum_{m=1}^{N} K_{N+n-m}D_m=-K_{N+n} \ , \tag{7}$$

$$\sum_{m=0}^{n} K_{n-m}D_m=C_n \ , \tag{8}$$

where $C_0=K_0$, $D_0=1$, and $n=1,\ldots,N$. All three methods will be applied in the following.

## III. THE INPUT OF THE MARCHENKO EQUATION

For the solution of the inverse scattering problem the complex reflection coefficient $R_-(q)$ must be known as a complex function of both positive and negative values of $q$ [cf. Eq. (1)]. However, usually only the reflectivity $r_-(q)=|R_-(q)|^2$ is measured, and this is done for momenta $q>0$. The reflection phase and the input for negative values of $q$ must therefore be obtained from additional information.

The phase problem has plagued structure research by x-ray, electron, or neutron scattering for decades.[31–40] In simulations, where the parameters of a preconceived model for the scattering profile are fitted to the data, the reflection phase is of course obtained as a result of the fit. However, recently some work on a model-independent determination of the reflection phase in one-dimensional scattering has appeared in the literature.[41–46] In the present work we shall not discuss this point, but regard the phase as given.

As to the reflection coefficient for negative values of $q$, it is, for real potentials, given simply by the complex conjugate of the reflection coefficient for positive values,[17]

$$R_-(-q)=R_-^*(q) \ . \tag{9}$$

However, for complex potentials this no longer holds. In order to obtain an analogous relation for this case, we consider the Jost solutions[17,19]

$$f_+(p,x)=\begin{cases}[e^{ipx}+R_-(p)e^{-ipx}]/T_-(p) & \text{for } x<0 \\ e^{i\bar{p}x} & \text{for } x\to\infty\end{cases} \tag{10}$$

and

$$f_-(q,x)=\begin{cases}e^{-iqx} & \text{for } x\to-\infty \ , \\ [e^{-i\bar{q}x}+R_+(q)e^{i\bar{q}x}]/T_+(q) & \text{for } x>0 \ ,\end{cases} \tag{11}$$

where $\bar{p}=\sqrt{p^2-V_s}$ is the wave number in the semi-infinite substrate, and similarly for $\bar{q}$. The quantity $R_+(q)$ is the right reflection coefficient, and $T_\mp(q)$ are the left and right transmission coefficients, respectively. Comparing the Wronskians between these two functions in the regions $x<0$ and $x>0$ with $p=-q$, we find

$$qR_-(-q)T_+(q)+\bar{q}R_+(q)T_-(-q)=0 \ . \tag{12}$$

In addition, the Wronskian between the functions[17,19]

$$f_-(-q,x)=T_-(q)f_+(q,x)-R_-(q)f_-(q,x) \tag{13}$$

and $f_+(-q,x)$ of Eq. (10) yields the relation

$$qR_-(-q)R_-(q)+\bar{q}T_-(q)T_-(-q)=q \ , \tag{14}$$

which replaces the law of conservation of current when the potential is complex. Combining Eqs. (12) and (14), we find, instead of Eq. (9),

$$R_-(-q)=\frac{R_+(q)}{R_-(q)R_+(q)-T_-(q)T_+(q)} \ . \tag{15}$$

We see that a knowledge of all coefficients $R_\mp(q)$ and $T_\mp(q)$ for $q>0$ is required in order to determine the left reflection coefficient $R_-(q)$ for $q<0$. The right transmission coefficient $T_+(q)$ can be replaced with the left coefficient $T_-(q)$ when use is made of

$$T_+(q)=\frac{\bar{q}}{q}T_-(q) \ , \tag{16}$$

which follows from a comparison of the Wronskians between functions (10) and (11) in the regions $x<0$ and $x>0$ with $p=q$.

## IV. NUMERICAL APPLICATIONS

In this exploratory work we give numerical solutions of the inverse scattering problem for known potentials, proceeding from simple schematic models to examples which describe actual physical situations. The direct solution of the Marchenko equation has been obtained by

the method of Galerkin[47,48] using $B$-spline polynomials.[48] The use of such piecewise polynomials to expand the kernel reduces the integral equation (2) to a linear equation for the expansion coefficients. This solution of the Marchenko equation is stable, and in all cases considered the potential obtained by direct solution of the Marchenko equation was found to coincide with the original potential. In the following we shall call this potential the Marchenko solution, in contrast to the approximate potentials obtained by the Neumann-series and Padé-approximant methods.

In general, however, solving the Marchenko equation directly is time consuming and requires a large computer memory. Therefore, two alternative approximate methods have also been investigated, the solution via a finite Neumann series and the method of Padé approximants. To facilitate further the efficiency of the calculation, the reflection coefficient as well as its Fourier transform were interpolated by the collocation method[49] using Hermite cubic splines.[50]

We note here that the reflection coefficient can be determined experimentally only up to a maximum value $q_c$. In the absence of any knowledge of $R_-(q)$ for $|q|>q_c$ the integration in the Fourier transform (1) is usually truncated at the cutoff momentum $q_c$. The ensuing integral $B(q_c;x)$

$$B(q_c;x)=\frac{1}{2\pi}\int_{-q_c}^{q_c} dq\, e^{-iqx}R_-(q) \quad \text{for } x>0 \tag{17}$$

contains oscillations of period $\pi/q_c$, and the Gibbs phenomenon[51] is expected to show up at sharp edges.

### A. A solvable Bargmann-type potential

We begin with a solvable potential of Bargmann type,[24] which has a form which is similar to that of the exponential profiles occurring in microemulsions[8] and in polymer segregation at the air/sample interface.[9] This potential is associated with a rational reflection coefficient, and has the form $V(x)=0$ for $x<0$ and

$$V(x)=\frac{2(b^2-a^2)a^2}{[b\sinh(ax)+a\cosh(ax)]^2} \quad \text{for } x>0\ . \tag{18}$$

The corresponding reflection coefficient and its Fourier transform are, respectively,

$$R(q)=\frac{(b^2-a^2)/2}{q^2+ibq-(b^2-a^2)/2} \tag{19}$$

and

$$B(x)=\frac{b^2-a^2}{2c}e^{-bx/2}\sin(cx) \quad \text{with } c=\sqrt{b^2-2a^2}/2\ . \tag{20}$$

The norm (5) entering in the condition for the convergence of the Neumann series is given by

$$\|B\|_x^2=\frac{(b^2-a^2)^2}{2c^2}\left[\frac{\sinh^2(bx)}{2c^2}-\frac{\mathrm{Re}\{(b-2ic)^2\sinh^2[(b+ic)x]\}}{(b^2+4c^2)^2}\right]. \tag{21}$$

Figure 1 illustrates this case for $a=-0.2$ nm$^{-1}$ and $b=0.4$ nm$^{-1}$. The Marchenko solution obtained from the reflection coefficient (19) coincides with the original potential. The potential corresponding to the first Neumann term, $-2dB(2x)/dx$, is also shown, together with the potentials provided by the first five, nine, and 15 Neumann terms ($M=4$, 8, and 14). It is seen that the Neumann series does not provide a satisfactory result, even when 15 terms are included. However, in the Padé-

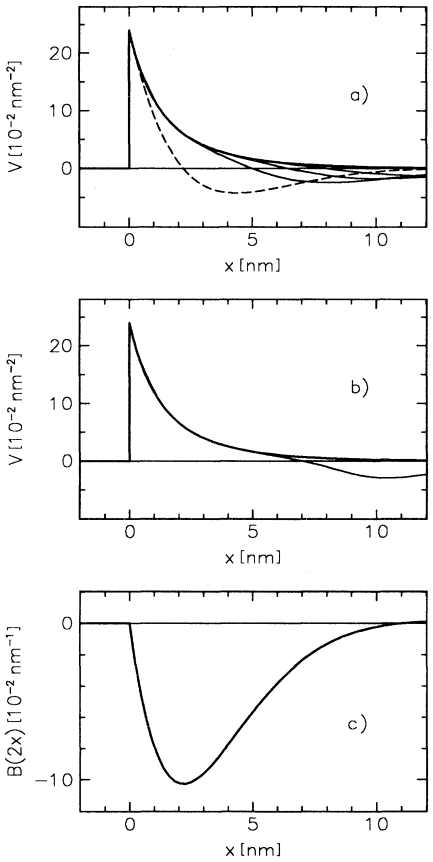


FIG. 1. Reconstruction of a Bargmann-type potential. (a) Potential (18) with $a=-0.2$ nm$^{-1}$ and $b=0.4$ nm$^{-1}$ (heavy solid curve) together with the Marchenko solution (not distinguishable from the original potential) and potentials corresponding to the Neumann series with $M=0$ (dashed curve) and $M=4$, 8, and 14 (thin solid curves, from left to right). (b) Potential (18) (heavy solid curve) together with the potentials corresponding to the (2,2), (4,4), and (7,7) Padé approximants (thin solid curves); only the (2,2) potential differs from the original one; the others coincide with the latter. (c) The input function $B(2x)$ corresponding to expression (20).

approximant method one does recover the original potential for $N \geq 4$. The convergence of the Neumann series can be checked with the help of condition (5). Using expression (21) in this condition, one finds that the Neumann ceases to converge for $x > 2.8$ nm. This is indeed the case, as is illustrated by Fig. 1(a).

### B. Step potential

For a pure step potential of height $V_s$ extending from $x=0$ to the right, the reflection coefficient is the Fresnel coefficient

$$R(q)=\frac{q-\bar{q}}{q+\bar{q}} . \tag{22}$$

This corresponds to scattering by an infinitely thick slab. The function $B(x)$ calculated with the help of Eq. (1) is $B(x)=0$ for $x<0$ and

$$B(x)=-\frac{2}{x}J_2(\sqrt{V_s}x) \quad \text{for } x>0 , \tag{23}$$

where $J_2$ is the Bessel function of order 2. The case of the step potential is illustrated in Fig. 2 for $V_s=25\times10^{-4}$ nm$^{-2}$. Again the Marchenko solution coincides with the original potential. Note that the input function $B(2x)$ oscillates, but leads to a straight-line solution for the potential $V(x)$.

The potentials corresponding to the different Neumann series are equal only to the beginning part of it; the potentials obtained in the Padé-approximant method reproduce the original potential out to larger distances than the Neumann series, but they also fail eventually. The analogous case with a cutoff $q_c=0.8$ nm$^{-1}$ is shown in Fig. 3. The oscillations of period $\pi/q_c=3.93$ nm are a consequence of the cutoff, and the Gibbs phenomenon is clearly visible at the edge.

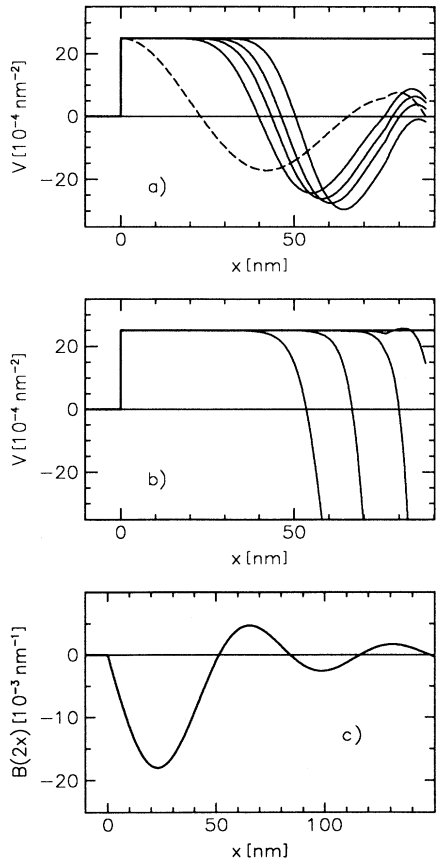


FIG. 2. Reconstruction of a step potential. (a) The original potential with $V_s=25\times10^{-4}$ nm$^{-2}$ (step function, heavy horizontal line), together with the Marchenko solution (identical with the former) and the solutions corresponding to the Neumann series with $M=0$ (dashed curve) and $M=4$, 6, 8, and 12 (thin solid curves, from left to right). (b) The original potential (heavy horizontal line) and the potentials corresponding to the (2,2), (3,3), (4,4), and (6,6) Padé approximants (thin solid curves, from left to right). (c) The input function $B(2x)$.

### C. Complex barrier with substrate

A homogeneous film on an infinitely thick substrate is represented by a square potential barrier in front of a step function. Surface-roughness effects may be simulated by a rounding off of the edges of the potential, while absorption will introduce an imaginary part. The input function $R(q)$ for $q<0$ has been obtained by solving the direct problem for $q<0$. The solution of the inverse scattering problem is illustrated in Fig. 4 for a potential of complex height $(50-i0.5)\times10^{-4}$ nm$^{-2}$, width 50 nm, and surface thickness 0.88 nm. The height of the substrate potential is $V_s=25\times10^{-4}$ nm$^{-2}$, and the cutoff parameter for the reflection coefficient is taken to be $q_c=8$ nm$^{-1}$. The Marchenko solution again coincides with the original po-

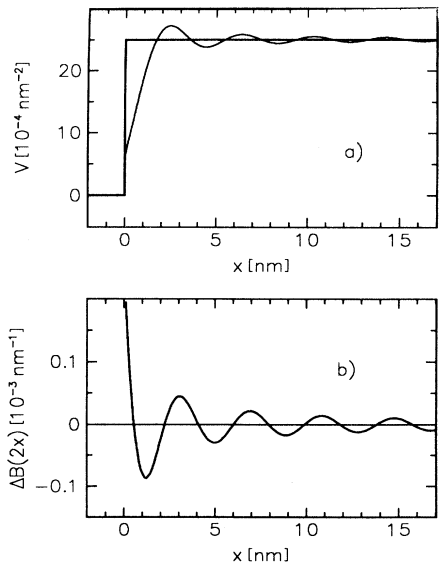


FIG. 3. The effect of a cutoff $q_c=0.8$ nm$^{-1}$ for the example of Fig. 2. (a) The Marchenko solution (thin curve). (b) The difference $\Delta B(2x)=B(2x)-B(q_c;2x)$.

tential; the approximate results using the Neumann series with 19 terms ($M=18$) and the (9,9) Padé approximant are also displayed.

The effect of lowering the cutoff to $q_c=1$ nm$^{-1}$ is shown in Fig. 5. It is seen that cutoff effects begin to become visible as small oscillations of the potential with period $\pi/q_c=3.14$ nm.

### D. Two double layers on a substrate

Finally, in Fig. 6 we present an example modeled on a realistic case, two double layers of iron and silver on an infinitely thick glass substrate. The potential height for iron is $V_{\mathrm{Fe}}=4\pi(806.6-i0.06)\times10^{-6}$ nm$^{-2}$, and for silver $V_{\mathrm{Ag}}=4\pi(348.2-i1.032)\times10^{-6}$ nm$^{-2}$. The potential height for glass is $V_{\mathrm{glass}}=4\pi440.0\times10^{-6}$ nm$^{-2}$.

Two values of the cutoff $q_c$ are considered. For a short cutoff, $q_c=1$ nm$^{-1}$, the Marchenko solution and the potential obtained with the help of a (9,9) Padé approximant are practically identical, and contain the expected oscillations of period $\pi/q_c=3.14$ nm. These are clearly seen in

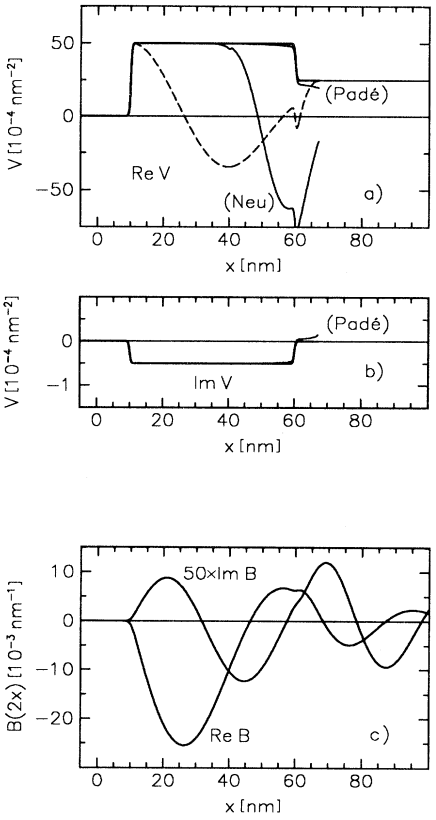


FIG. 4. Reconstruction of a complex potential with diffuse edges representing a homogeneous film on an infinitely thick substrate with surface and interface roughness. The complex barrier height is $(50-i0.5)\times10^{-4}$ nm$^{-2}$, the width is 50 nm, and the surface and interface thickness is 0.88 nm. The potential representing the substrate has the height $V_s=25\times10^{-4}$ nm$^{-2}$. (a) and (b) are the real and imaginary parts of the original potential (heavy solid curve) together with the Marchenko solution (identical with the former), and potentials corresponding to the Neumann series with $M=0$ (dashed curve) and 18, and the (9,9) Padé approximant (thin solid curves); note the difference in scale for the real and imaginary parts; in the imaginary part only the original and the Padé approximant are shown, since the Neumann-series method yields no meaningful results. (c) The complex input function $B(2x)$.

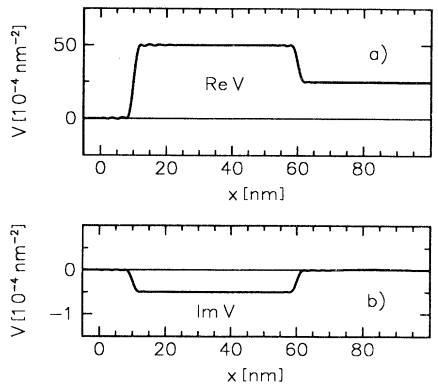


FIG. 5. The effect of a cutoff $q_c=1$ nm$^{-1}$ on the Marchenko solution for the example of Fig. 4.

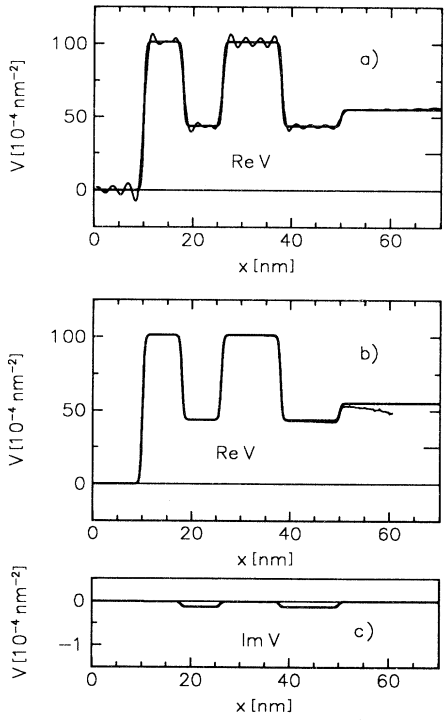


FIG. 6. Reconstruction of an iron-silver double-layer structure on a glass substrate. (a) The real part of the original potential (heavy curve) and its reproduction by the Marchenko solution with the cutoff $q_c=1$ nm$^{-1}$ (thin curve). The reconstruction via a (9,9) Padé approximant with the same cutoff coincides with the Marchenko solution. (b) The real part of the original potential and its reconstruction via a (9,9) Padé approximant with the cutoff $q_c=6$ nm$^{-1}$. (c) The imaginary part of the original potential and its reproduction by the Marchenko solution with a cutoff $q_c=1$ nm$^{-1}$.

the real part [cf. Fig. 6(a)] but less so in the imaginary part [cf. Fig. 6(c)]. After averaging over these oscillations the Marchenko solution is seen to reproduce the original potential.

For a long cutoff $q_c = 6\ \mathrm{nm}^{-1}$, a sufficiently accurate Marchenko solution requires a great numerical effort. Therefore, we have restricted ourselves to employing the Padé-approximant method. It is found that the potential corresponding to the (9,9) Padé approximant reproduces the original potential to good accuracy [cf. Fig. 6(b)].

## V. SUMMARY

We have given examples of the implementation of general inverse scattering theory for a model-independent analysis of neutron specular reflection experiments. Various scattering-length density profiles of physical interest have been reconstructed exactly by solving the Marchenko integral equation, which is the central equation of the one-dimensional inverse scattering problem. Approximate procedures of solutions have also been considered, and the effect of data limitation, such as, e.g., a cutoff in the momentum transfer, has been discussed. The application of such inversion methods appears to be feasible in principle. The main difficulty which remains to be solved in a practical manner is the phase problem, i.e., the determination of the reflection phase from experimental information. Increased efforts have been made to solve this important problem in the recent literature.[41–46]


*Deceased.

[1]V. F. Sears, *Neutron Optics* (Oxford University Press, Oxford, 1989).

[2]T. P. Russel, Mater. Sci. Rep. **5**, 171 (1990).

[3]J. Penfold and R. K. Thomas, J. Phys. Condens. Matter **2**, 1369 (1990).

[4]G. Felcher, Proc. SPIE **983**, 2 (1988).

[5]*Workshop on Methods of Analysis and Interpretation of Neutron Reflectivity Data,* edited by G. Felcher and T. P. Russel [Physica B **173**, 1 (1991)].

[6]J. B. Pendry, K. Heinz, and W. Oed, Phys. Rev. Lett. **61**, 2953 (1988).

[7]Xiao-Lin Zhou, G. P. Felcher, and Sow-Hsin Chen, Physica B **173**, 167 (1991).

[8]Xiao-Lin Zhou, Lay-Theng Lee, Sow-Hsin Chen, and R. Strey, Phys. Rev. A **46**, 6479 (1992).

[9]Xiao-Lin Zhou and Sow-Hsin Chen, Phys. Rev. E **47**, 3174 (1993).

[10]Sow-Hsin Chen, Xiao-Lin Zhou, and B. L. Carvalho (unpublished).

[11]D. L. Worcester, Physica B **173**, 139 (1991).

[12]T. M. Roberts, Physica B **173**, 157 (1991).

[13]M. Stamm, in *Physics of Polymer Surfaces and Interfaces,* edited by I. C. Sanchez and L. E. Fitzpatrick (Butterworth-Heinemann, Boston, 1987), p. 163.

[14]X.-L. Zhou, S.-H. Chen, and G. P. Felcher, in *Inverse Problems in Scattering and Imaging,* edited by M. Bertero and E. R. Pike (Hilger, Bristol, 1992), p. 109.

[15]I. Kay, Comm. Pure Appl. Math. **13**, 371 (1960).

[16]Z. S. Agranovich and V. A. Marchenko, *The Inverse Problem of Scattering Theory* (Gordon and Breach, New York, 1963).

[17]K. Chadan and P. C. Sabatier, *Inverse Problems in Quantum Scattering Theory,* 2nd ed. (Springer, Berlin, 1989).

[18]F. Calogero and A. Degasperis, *Spectral Transform and Solitons* (North-Holland, Amsterdam, 1982), Vol. 1.

[19]A. Cohen and T. Kappeler, Indiana Univ. Math. J. **34**, 127 (1985).

[20]H. Leeb and D. Leidinger, Few Body Syst. **6**, 117 (1992); R. M. Adam, H. Fiedeldey, S. A. Sofianos, and H. Leeb, Nucl. Phys. A **559**, 157 (1993).

[21]M. Coz, J. Kuberczyk, H. V. von Geramb, and J. D. Lumpe, Z. Phys. A **326**, 345 (1987); **328**, 265 (1987); Th. Kirst, K. Amos, L. Berge, M. Coz, and H. V. von Geramb, Phys. Rev. C **40**, 912 (1989).

[22]A. K. Jordan and H. D. Ladouceur, Phys. Rev. A **36**, 4245 (1987); A. K. Jordan and S. Lakshmanasamy, J. Opt. Soc. Am. A **6**, 1206 (1989). A. K. Jordan, L. S. Tamil, and J. Xia, in *Inverse Problems in Scattering and Imaging* (Ref. 14), p. 228.

[23]K. R. Pechenick and J. M. Cohen, J. Math. Phys. **22**, 1513 (1981); **24**, 406 (1983); Phys. Lett. **82A**, 156 (1981).

[24]R. Lipperheide, G. Reiss, H. Fiedeldey, S. A. Sofianos, and H. Leeb, Physica B **190**, 377 (1993).

[25]R. Lipperheide, G. Reiss, H. Fiedeldey, S. A. Sofianos, and H. Leeb, Surf. Sci. **307-309**, 901 (1994).

[26]A. R. Osborne, A. Provenzale, and L. Bergamasco, Nuovo Cimento **5C**, 597 (1982).

[27]M. Corvi, in *Inverse Problems in Scattering and Imaging* (Ref. 14), p. 411.

[28]P. E. Sacks, Wave Motion **18**, 21 (1993).

[29]G. A. Baker, Jr. and P. Graves-Morris, in *Encyclopedia of Mathemathics and its Applications,* edited by G.-C. Rota (Addison-Wesley, Reading, MA, 1981), Vols. 13 and 14.

[30]W. H. Press, S. A. Teukolsky, W. T. Vetterling, and B. P. Flannery, *Numerical Recipes in Fortran,* 2nd ed. (Cambridge University Press, Cambridge, 1992), Sec. 5.12.

[31]J. M. Cowley, *Diffraction Physics* (North-Holland, Amsterdam, 1975).

[32]G. Bricogne, in *Maximum Entropy in Action,* edited by B. Buck and V. A. Macaulay (Clarendon, Oxford, 1991).

[33]*Crystallographic Computing 5,* edited by D. Moras, A. Podjarny, and J. C. Thierry (Oxford University Press, Oxford, 1991).

[34]M. J. Buerger, *Crystal Structure Analysis* (Wiley, New York, 1967).

[35]Xiao-Lin Zhou, Sow-Hsin Chen, and G. P. Felcher, in *Inverse Problems in Scattering and Imaging* (Ref. 14), p. 109.

[36]R. E. Burge, M. A. Fiddy, A. H. Greenaway, and G. Ross, Proc. R. Soc. London Ser. A **350**, 191 (1976).

[37]F. Rieutord, J. J. Benattar, R. Rivoira, Y. Lepatre, C. Blot, and D. Luzet, Acta Crystallogr. Sec. A **45**, 445 (1989).

[38]E. Spiller, Rev. Phys. Appl. **23**, 1687 (1988).

[39]E. J. Kramer, Physica B **173**, 189 (1991).

[40]H. A. Hauptmann, Rep. Prog. Phys. **54**, 1427 (1991).

[41]W. D. Dozier, J. M. Carpenter, and G. P. Felcher, Bull. Am. Phys. Soc. Ser. II **36**, 772 (1991).

[42]M. V. Klibanov and P. E. Sacks, J. Math. Phys. **33**, 3813 (1992).

[43]P. E. Sacks (unpublished).

[44]W. J. Clinton, Phys. Rev. B **48**, 1 (1993).

[45]D. S. Sivia, W. A. Hamilton, G. S. Smith, T. P. Rieker, and R. Pynn, Jr., Appl. Phys. **70**, 732 (1991); D. S. Sivia, W. A. Hamilton, and G. S. Smith, Physica B **173**, 121 (1991); W. Lesslauer and J. K. Blaisie, Acta Crystallogr. Sec. A **27**, 456 (1971).

[46]H. Fiedeldey, R. Lipperheide, H. Leeb, and S. A. Sofianos, Phys. Lett. A **170**, 347 (1992).

[47]V. G. Galerkin, Vestn. Inzh. **1**, 897 (1915).

[48]H.-J. Reinhardt, *Analysis of Approximation Methods for Differential and Integral Equations,* Springer Series on Applied Mathematical Sciences Vol. 57 (Springer, Berlin, 1985).

[49]M. G. Cox, J. Inst. Math. Appl. **10**, 134 (1972); C. de Boor, *A Practical Guide to Splines,* Springer Series on Applied Mathematical Sciences Vol. 27 (Springer, Berlin, 1978).

[50]P. Lancaster and K. Salkauskas, *Curve and Surface Fitting* (Academic, New York, 1986); G. L. Payne, in *Models and Methods in Few-Body Physics,* edited by L. S. Ferreira, A. C. Fonseca, and L. Streit, Lecture Notes in Physics Vol. 273 (Springer, Berlin, 1987).

[51]P. M. Morse and H. Feshbach, *Methods of Theoretical Physics* (McGraw-Hill, New York, 1953), p. 745.